Journal of Adhesion Science and Technology

Publication details, including instructions for authors and subscription information:
http://www.tandfonline.com/loi/tast20

Janus-faced micro and nanopillars for geometry and surface chemistry controllable bioinspired dry adhesives

Yudi Rahmawan[abc], Hyunsik Yoon[d], Myoung-Woon Moon[b], Hak-Geun Jeong[e] & Kahp-Yang Suh[a]

[a] Division of WCU Multiscale Mechanical Design, School of Mechanical & Aerospace Engineering, Seoul National University, Seoul, 151-744, Republic of Korea.

[b] Interdisciplinary Fusion Technology Division, Korea Institute of Science and Technology, Seoul, 130-650, Republic of Korea.

[c] Department of Materials Science and Engineering, University of Pennsylvania, Philadelphia, 19104, USA.

[d] Department of Chemical Engineering, Seoul National University of Science & Technology, Seoul, 139-743, Republic of Korea.

[e] Electrics & Lighting Research Center, Korea Institute of Energy Research, Daejon, 305-343, Republic of Korea.

Published online: 10 Aug 2012.

To cite this article: Yudi Rahmawan, Hyunsik Yoon, Myoung-Woon Moon, Hak-Geun Jeong & Kahp-Yang Suh (2014) Janus-faced micro and nanopillars for geometry and surface chemistry controllable bioinspired dry adhesives, Journal of Adhesion Science and Technology, 28:3-4, 367-386, DOI: 10.1080/01694243.2012.693825

To link to this article: http://dx.doi.org/10.1080/01694243.2012.693825

Journal of Adhesion Science and Technology, 2014
Vol. 28, Nos. 3–4, 367–386, http://dx.doi.org/10.1080/01694243.2012.693825

Janus-faced micro and nanopillars for geometry and surface chemistry controllable bioinspired dry adhesives

Yudi Rahmawan[a,b,c], Hyunsik Yoon[d], Myoung-Woon Moon[b], Hak-Geun Jeong[e] and Kahp-Yang Suh[a]*

[a]*Division of WCU Multiscale Mechanical Design, School of Mechanical & Aerospace Engineering, Seoul National University, Seoul, 151-744, Republic of Korea;* [b]*Interdisciplinary Fusion Technology Division, Korea Institute of Science and Technology, Seoul, 130-650, Republic of Korea;* [c]*Department of Materials Science and Engineering, University of Pennsylvania, Philadelphia 19104, USA;* [d]*Department of Chemical Engineering, Seoul National University of Science & Technology, Seoul, 139-743, Republic of Korea;* [e]*Electrics & Lighting Research Center, Korea Institute of Energy Research, Daejon, 305-343, Republic of Korea*

(*Received 4 May 2011; final version received 18 July 2011; accepted 31 August 2011*)

Janus-faced pillar structures are a new class of bioinspired dry adhesives based on the exploitation of unique physical and chemical properties when two different materials are placed on two opposite faces. Using Janus-faced high aspect ratio (HAR) pillars, it is possible to control the geometry and surface chemistry that are key factors in designing gecko-inspired artificial dry adhesives with high performance. In this review, first, we revisit the conventional fabrication techniques for homogeneous, angled HAR structures. Second, we present the fabrication methods for Janus-faced micro and nanopillars via physical and chemical modification of one of the faces. Third, we discuss the geometric features of Janus-faced structures with bending mechanisms of the pillars and the selection of contacting faces. Finally, we cover the theoretical and practical viewpoints of adhesion behavior with a particular focus on the role of work of adhesion, tilt angle, and adhesion hysteresis. We emphasize that Janus-faced structures potentially provide powerful systems to control anisotropic adhesion behavior by taking advantage of both physical and chemical aspects of the angled structures.

Keywords: Janus-faced structures; angled nanopillars; dry adhesion; e-beam irradiation; ion beam irradiation; oblique metal deposition; surface energy; adhesion hysteresis

1. Introduction

It has been intensively studied that many natural species such as insects (e.g. flies and bugs), arachnids (e.g. spiders), and small reptiles (e.g. geckos, anoles, or skinks) use their fibrillar structures for adhesion function [1,2]. Among them, gecko foot hair has been an attractive topic to many researchers due to its fabulously high dry adhesion strength and locomotion ability. The natural design of Tokay gecko (*Gekko gecko*) toe consists of structural hierarchy, starting from millimeter scale overlapping lamellae. The outer part of surface contacting lamellae is made of long, high aspect ratio (HAR) fibrillar structures (termed 'setae') with average 110 μm height and 5 μm diameter. The end of a seta is branched into 100–1000 nano-hairy structures (termed 'spatulae') with average height of 2 μm and diameter of 200 nm

*Corresponding author. Email: sky4u@snu.ac.kr

[1,3,4]. The material of gecko foot hair is made from relatively rigid, hydrophobic material β-keratin (modulus of elasticity, $E = 1$–3 GPa, water wetting angle of 128° [3,5]), including the claw in each toe for mechanical interlocking. With the features given above, the gecko has the ability to cling to almost all kinds of surfaces regardless of roughness, to detach effortlessly from the surfaces with a speed of >1 m/s, and to self-clean their pads [6–8].

Since the discovery of gecko's adhesion system, the research in gecko-inspired dry adhesives has been diverged into various topics including the adhesion mechanisms from both physical and chemical viewpoints, the responsible forces and their contribution to the total adhesion force, interactions between HAR micro and nanostructures, and modeling and technological applications. Especially, it is worthwhile noting that the HAR fibrillar structures of gecko toe either at seta or spatula level are angled to a position from the adhering surface normal. The underlying mechanisms have been intensively studied and now it is accepted that the angled, HAR fibrillar structures help increase the directionality of adhesion force (i.e. high adhesion force in shear direction and low adhesion in opposite direction) and reduce the effective Young's modulus closer to the tacky region in the Dahlquist criterion for tackiness [9–12]. Autumn and co-workers showed that the tilt angle of a rod is critical to determine the effective modulus of elasticity [9]:

$$E_{\text{eff}} = \frac{3EID\sin(\phi)}{L^2\cos^2(\phi)[1 \pm \mu\tan(\phi)]} \tag{1}$$

here, E *is* the modulus of elasticity, I is the area moment of inertia, D is the hair density, ϕ is the tilt angle of rod, L is the rod length, and μ is the friction coefficient. The ± sign in Equation (1) indicates, respectively, the shear direction along and against the rod orientation. It can be easily expected that the surface becomes more compliant as the shear force is applied along the natural orientation of gecko setae sloping angle to surface normal. A more specific number from Equation (1) has been shown that natural-angled gecko seta of β-keratin material with $E \cong 1$ GPa has $E_{\text{eff}} \cong 10^5$ Pa, which is close to the value of the Dahlquist criterion for tackiness [9]. In addition to the advantages of increasing adhesion force uni-directionally by lowering E_{eff}, the angled structures would enhance the interfacial crack propagation when the detachment is initiated between the toe pad and substrate [13–15]. In this case, assuming that the elastic energy stored in each spatula does not change during pull off, and the contact between spatula and solid surface represents a contact between two perfectly flat solid surfaces, the normal pull-off force is given by $F_{\perp} = F\sin\theta = \dfrac{\Delta\gamma B\sin\theta}{1-\cos\theta}$ [13]. Here, F is the pull-off force, θ is the the peel angle, B is the the width of spatula, and $\Delta\gamma$ is the change in the interfacial energy (per unit area) when perfectly flat surfaces of the two solids are brought into contact. Indeed, the gecko is believed to roll the toe to break the adhesion between the toe pad and substrate for easy detachment [13].

In order to utilize the directional, smart adhesion behavior mentioned above, many researchers have been trying to fabricate artificial dry adhesive structures either in single scale structure or multiscale hierarchical structures with various materials and fabrication methods. From the viewpoint of conformal contact, it is critical to design the end tip of fibrillar structures as the adhesion force is linearly proportional to the size of contacting area. Accordingly, many spatula shapes such as flat, mushroom, etc have been employed and analyzed in depth by several research groups to optimize the adhesion force [16–18]. Interestingly, the shape effect may become insensitive, when the diameter of fibrillar structures is scaled down to about 100 nm [11,19]. Therefore, the design of artificial dry adhesives using fibrillar structures

below or close to 100 nm can be focused on the work of adhesion and increasing the contact length by forming angled pillar structures.

Motivated by the importance of tuning the geometry and surface chemistry in designing dry adhesives, a new class of unique and robust dry adhesives has been introduced, which is termed 'Janus-faced pillar structures.' Here, one side or face of the pillar is physically or chemically altered to have remarkably distinct behavior from the other side. The properties of Janus-faced pillar structures can be exploited in various ways to obtain optimum geometry and surface chemistry of dry adhesive materials. In parallel, the actual governing forces and structural design issues have been recently established from both physical and chemical viewpoints, thereby widening applications of the Janus-faced structures [5,16,20,21].

In this brief overview, we present the recent developments for exploiting the unique adhesion properties of Janus-faced structures. In the first part, we review the fabrication methods for homogeneous, angled HAR structures in micro or nanoscale with a single material. The second part discusses the fabrication methods for Janus-faced structures in the form of angled pillars in micro or nanoscale. Finally, we discuss the theoretical aspects of the adhesion properties of Janus-faced structures. This review will be a useful guide for scientists and engineers who want to utilize the Janus-faced structures in an artificial dry adhesive system.

2. Homogeneous, angled HAR structures

Homogeneous structures are comprised of monolithic objects having uniform properties throughout the body. In angled structures, the tilt angle is defined as the tangential angle at the tip of structures and is typically measured from the side view of scanning electron microscopy (SEM) images of the structures. Throughout the review, we classify pillars into micro and nanopillars based on their diameter. Specifically, micropillars are pillars with diameters on the order of several micrometers to several hundreds of micrometers; Nanopillars are pillars with sub-micrometer diameters (a few tens of nanometers to several hundreds of nanometers). The fabrication of homogeneous, angled HAR structures is summarized below.

2.1. Fabrication of homogeneous, angled HAR micropillars

To fabricate homogeneous, angled HAR structures, an advanced conventional photolithography process was demonstrated. Aksak and co-workers [22] used inclined optical lithography and polymer micromolding technique. In this process, the inclined microfiber arrays were made from SU-8 photoresist with pre-baked backup layer on glass wafer to prevent delamination during microfiber removal. The aspect ratio of the microfibers was determined from the thickness of SU-8 photoresist (SU-8 2025, MicroChem, MA, USA). The angled microfibers made from polyurethane (PU) can be simply obtained by tilting the glass wafer during UV exposure. A further development of the same process has been shown by integrating mushroom [18] and spatula [23] tips. Using this method, the tilt angle of microfibers can be tuned from 0° to 18° on large area up to 8 inch diameter of glass wafer.

Reddy and co-workers [24] used a shape memory thermoplastic elastomer to make angled micropillars. Here, an elastomer with pre-patterned structures was heated at a temperature higher than the glass transition temperature, $T > T_g$ under the application of deformation shear force. The sample was then cooled to below T_g while maintaining the deformed state of the shape memory elastomer. On angled, micropillars thus formed with an angle of about 45°, unlike what is expected, the adhesion force was somewhat lower compared to that of vertical pillars due to the loss of contact area in the angled geometry. Another way to make angled micropillars was reported by Santos and co-workers [11]. They used a triple-mold assembly

in the process, which consisted of a bottom mold to provide flat base for micropillars, a middle mold with angled holes and bevel end for angled tips, and a top mold to cast the liquid polymer into angled surfaces. A uniform, well-defined structure of directional polymer stalks was achieved using PU after micromolding with the assembly.

The SEM images of homogeneous, angled HAR micropillars using the above techniques are shown in Figure 1. It is noted that the fabrication of angled, HAR pillars, even at microscale level, is not simple and straightforward and a specific modification would be required to modify the conventional photolithographic or soft lithographic process [25,26]. Furthermore, there are also potential limitations in materials selection, resolution in terms of size and shape, maximum tilt angle, and uniformity over large-area coverage. A sophisticated process, which is capable of fabricating angled, HAR micropillars with well-tuned geometry is still a technological challenge.

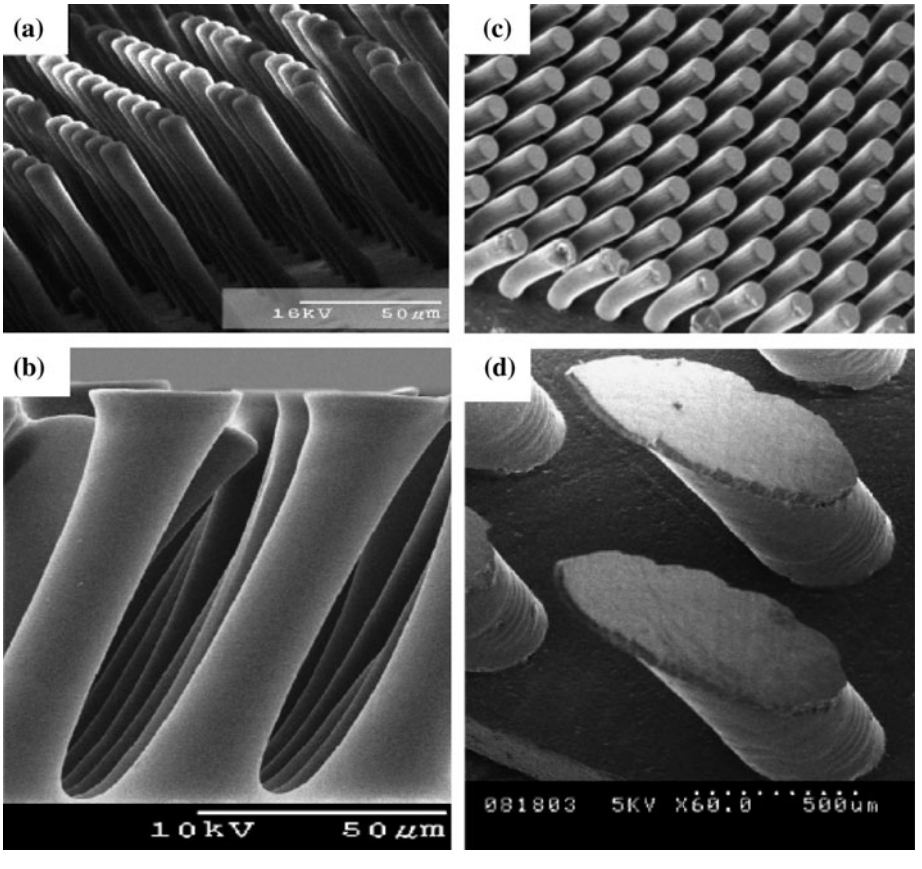

Figure 1. SEM images of various homogeneous, angled HAR micropillars fabricated by advanced lithographic process. (a) PU with round tips. Reprinted from [22]. (b) PU with spatula tips. Reprinted from [23]. (c) A shape memory thermoplastic elastomer, Tecoflex 72D (Thermedic Polymer Products, MA USA), with angled structures resulted from deformation force. Reprinted from [24]. (d) PU with directional stalk structures. Reprinted from [11].

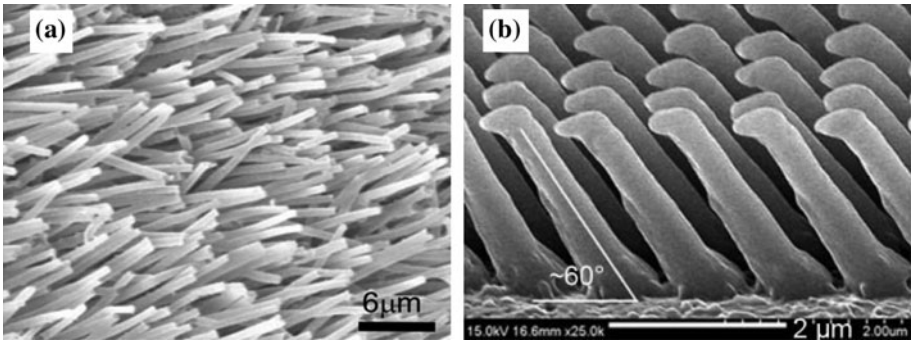

Figure 2. SEM images of homogeneous, angled HAR nanopillars by advanced lithographic process. (a) PP fabricated by replica molding from negative Si mold with vertical etching followed by rolling process. Reprinted from [27]. (b) PUA fabricated by replica molding from negative Si mold with angled etching. Reprinted from [28].

2.2. Fabrication of homogeneous, angled HAR nanopillars

The fabrication of homogeneous, angled HAR pillars in nanoscale is even more challenging compared to that of angled micropillars. The first method to make angled HAR nanopillars for dry adhesive applications was reported by Lee and co-workers [27], where a pre-patterned polypropylene (PP) with nanoscale vertical pillars was initially fabricated. The vertical nanopillars were made by casting PP onto polycarbonate (PC) filter with 0.6 μm pores under vacuum at 200 °C. After the removal of PC in methylene chloride, an array of fairly uniform vertical nanopillars was achieved. Next, the rolling process was applied onto the vertical nanopillars, resulting in angled nanopillars. Recently, Jeong and co-workers used an angled plasma etching process to make angled nanoholes on silicon on insulator (SOI) wafer [28]. Here, to uniformly direct the path of ions perpendicularly to the sample's surface normal during reactive ion etching (RIE) process, a Faraday cage was installed surrounding the sample. By placing the SOI wafer in a certain angle, it was possible to etch away the exposed part of the SOI wafer to obtain a Si mold with angled nanoholes. With the aid of controlled wet etch and etch stop of the underlying SiO_2 layer, it was also possible to modify the tip of nanoholes into a flat structure. The SOI wafer mold was used in replica molding using polyurethane acrylate [PUA]). The SEM images of representative homogeneous, angled HAR nanopillars are shown in Figure 2.

The difficulties in the fabrication of nanoscale-angled HAR pillars are attributed to the optical limit of photolithography used to make the master mold, which is also considered as an expensive process for large-scale production. Furthermore, pillars of single material composition are also potentially limited due to the lack of various functional properties from geometrical, chemical, and electrical aspects.

A summary of the properties of homogeneous, angled HAR pillars in micro and nanometer scales is presented in Table 1. It is noted that the maximum tilt angle of microscale pillars usually is limited to about 30° due in part to the clumping problem between the homogeneous, angled HAR micropillars after treatment [22] or to the shadowing problem of beam irradiation to create instability in Janus-faced micropillars [29]. In contrast, similar problems were not encountered in nanopillars, where the maximum tilt angle could be tuned to nearly 90°. From the viewpoint of adhesion force, it is apparent that adhesion force will be higher in nanopillars compared to that of micropillars due to the increased actual contact area [2]. Spe-

Table 1. A summary of properties of angled HAR micro and nanopillars.

Materials (modulus)	Fabrication methods	Spatula tips	Dia. (μm)	AR	Max. tilt angle (°)	Tensile adhesion strength (N/cm^2)	Shear adhesion strength (N/cm^2)	Preload (N/cm^2)	Refs.
PU (300 kPa)	Replica molding	No	380	~3	20	0.26	0.26	0.25	[11]
PU (3 MPa)	Replica molding, liquid polymer dipping and curing	Yes	35	~2.5	33	NI	10	NI	[18]
PU (3 MPa)	Inclined photolithography	No	25	3	18	~0	9	NI	[22]
PDMS (20 MPa)	Broad ion beam irradiation	No	10	3	32	1	NI	NI	[29]
PP (1GPa)	Replica molding, roll pressing	No	0.6	3.3	45	~0	2.25	<0.1	[27]
PU (20 MPa)	Replica molding, heating with deformation force	No	0.5–50	20	45	3	NI	NI	[24]
Si (185GPa)	RIE, oblique deposition	No	0.5	12	52	NI	NI	NI	[42]
PUA (19.8 MPa)	Angled etching, Replica molding	Yes	0.35	8	60	14	26	0.3	[28,53]
PUA (19.8 MPa)	AAO replica molding, oblique metal deposition	No	0.045–0.2	1.8–15	20	NI	6.5	0.1	[34]
PUA (19.8 MPa)	E-beam irradiation	No	0.1	10	30	NI	11	0.3	[31]
PUA (19.8 MPa)	Oblique metal deposition	No	0.1	10	20	NI	31	0.3	[32,43]
PUA (19.8 MPa)	Broad ion beam irradiation, surface energy modification	No	0.1	10	80	NI	120	0.3	[30]

Notes: NI – Not indicated.
Preload – Average normal force per unit area of dry adhesive patch applied before shear adhesion test to make conformal contact. The tensile load is not exerted during shear adhesion test.

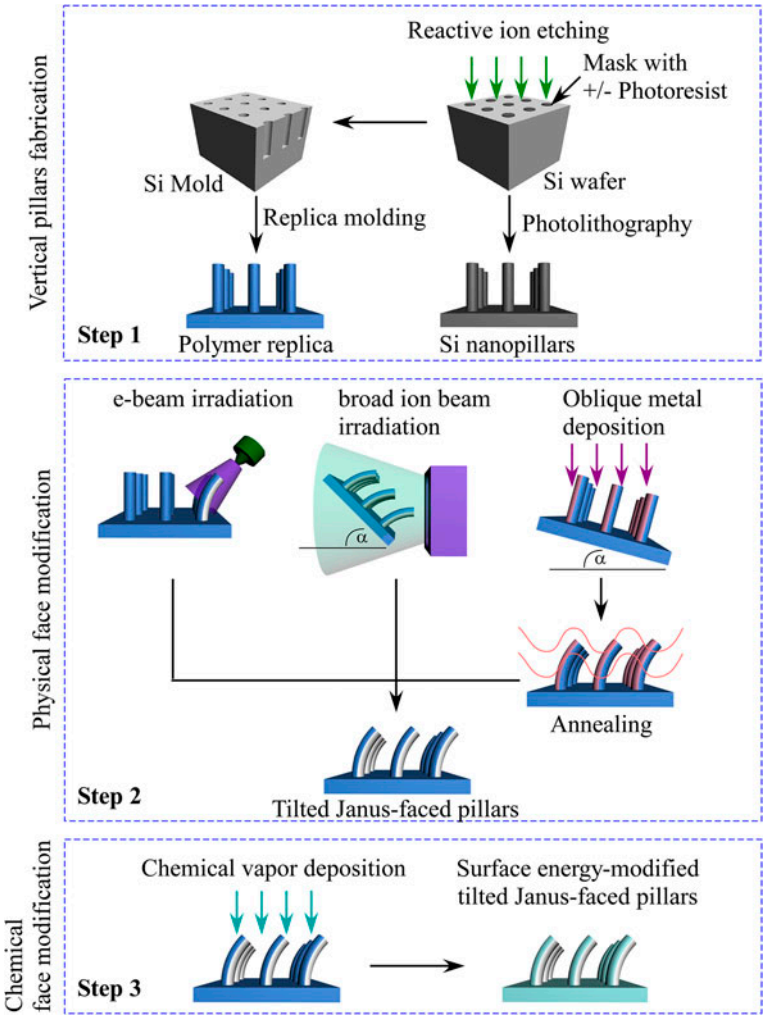

Figure 3. Scheme of fabrication routes for Janus-faced pillars with physical and/or chemical modification.

cific values for the comparison of adhesion strengths for nano and microscale pillars are listed in Table 1, suggesting that the adhesion strength differs by an order of magnitude. For example, the adhesion strength of angled micropillars can be only to 10 N/cm^2 [18] while angled nanopillars can reach 120 N/cm^2 [30]. In the table, we have averaged the preloading force per unit area. Here, preload is a normal load applied to dry adhesive patch to make conformal contact between pillars and counter surface [28]. In general, the preload is not exerted during the application of shear adhesion force. The detailed effect of tilt angle and surface chemistry on the adhesion force is explained in subsequent sections.

3. Janus-faced structures and their fabrication methods

The word 'Janus' comes from the Roman god as the custodian for the universe who had two opposing faces. In the area of dry adhesives, it was recently proposed that Janus-faced structures can be utilized as an efficient system for dry adhesive material due to their unique structural features [31,32]. Since the introduction of the concept, a series of new processes have been developed for their better performance as an artificial dry adhesive [29,30,33,34]. Here, we define Janus-faced structures as a new class of dry adhesive with the contrasting behaviors of two opposing, vertically standing faces.

The current patterning technology has enabled one to obtain various HAR vertical structures including projection lithography [35], scanning beam lithography (e-beam [36,37], focused ion beam [38,39]), and unconventional processes such as soft lithography [40,41]. Nonetheless, the fabrication of angled HAR micro and/or nanostructures composed of a single material is still limited due to several obstacles as explained in the previous section. To tackle some of the limitations, several alternative ways of preparing Janus-faced structures have been introduced either in single step or multistep methods. In general, Janus effect can be utilized by bending one of the faces with a physical treatment to the existing vertical pillars. During the process, one side of the as-prepared vertical pillars is physically altered, resulting in the transformation of vertical structures into angled ones together with a change in mechanical properties such as Young's modulus and stiffness.

Here, we classify physical modification into three types: e-beam irradiation [31,33], oblique metal deposition [32,34,42,43], and broad ion beam irradiation [29,30], which is schematically shown in Figure 3. In all cases, the initial vertical pillars either in micro or nanoscale can be prepared using the conventional process (i.e. photolithographic and/or soft lithographic processes by replica molding) [25,26]. Subsequently, the vertical pillars are exposed to the physical treatment and become slanted to a certain angle with respect to the bottom substrate. If special surface functionalities need to be added, the angled pillars can be further treated by post chemical vapor deposition using oxygen ion beams or physical process using thin film deposition. An example of the combination of both oblique Ar-ion beam irradiation and post-oxygen ion beam treatment was recently investigated to make angled nanopillars as well as to tune surface energy of the angled pillars [30]. Below are specific techniques to fabricate angled micro and nanopillars on the basis of physical modification.

3.1. E-beam irradiation

The first physical modification method was introduced by utilizing e-beam irradiation emitted from an electron gun in a vacuum chamber. Kim and co-workers suggested e-beam irradiation using commercial SEM system to make angled nanopillars [31,33]. The angled nanopillars with tilt angle from 0° to 30° can be obtained by simply tilting the sample to the e-beam direction. Since the effective coverage area of e-beam is relatively narrow (about $3 \times 3\,\mu m^2$) in the SEM system, it requires relatively long time process (up to several hours to bend 1 cm^2 of nanopillars dry adhesive patch) and good technical skills to obtain uniformly angled structures. The fixed e-beam irradiation duration and acceleration voltage were used as basic parameters. The relationship between tilt angle and irradiation time was reported to be linear up to certain irradiation time [31].

As for the bending mechanism, the electron beam with short scanning distance in the SEM system would carry electrons with lower energy. Therefore, it is not easy to produce a scissoring effect or etching on the surface to create carbonaceous or silica-like stiff skin on

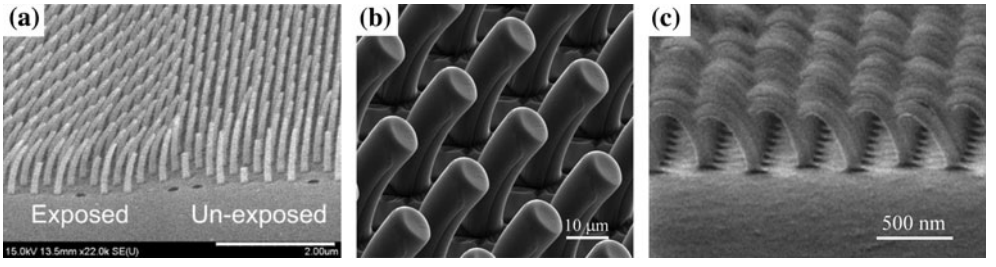

Figure 4. SEM images of angled Janus-faced pillars fabricated from vertical pillars: (a) nanoscale HAR PUA pillars bent by e-beam irradiation. The Janus-faced pillars are shown as bent pillars in the exposed area while pillars in the unexposed area remain vertical. Reprinted from [31]. (b) Microscale HAR PDMS pillars bent by broad ion beam irradiation. Reprinted from [29]. (c) Nanoscale HAR PUA pillars bent by oblique metal deposition. Reprinted from [32].

the surface. The possible reaction is, therefore, chemical decomposition, where the bending process is material and size dependent. In the case of PUA which is composed of PU backbone with acrylate groups [44], the C=O units will be decomposed into COOH at the first stage, and then followed by CO_2 gas formation at the next stage under the e-beam irradiation [45]. The consequence of this process is the reduction in volume of the e-beam irradiated part. Finally, the volume shrinkage of the irradiated polymer face made the vertical pillars to bend towards the direction of e-beam irradiation.

An example of angled nanopillars made by the e-beam irradiation can be seen in Figure 4(a). Here, the distinct difference can be seen between exposed and unexposed regions to the e-beam. The low productivity of using this method has been restricting the widespread use for large-area dry adhesives.

3.2. Broad ion beam irradiation

To address the low speed of the e-beam irradiation, broad ion beam irradiation utilizes surface-ions interactions to bombard the target surface over a large area up to meterscale which depends on the ion gun size. To physically change the surface properties without any chemical reactions, the ions from inert gas like argon are usually used. To conduct broad ion beam irradiation process, a typical hybrid ion beam system with high vacuum chamber ($P \cong 10^{-5}$ Pa) can be used [29,46]. Specifically, argon gas is introduced into an end-Hall type ion gun, a permanent magnet ion source in the anode to produce ion beam with a controllable energy. The path of ions is directed towards the sample position in the cathode assisted by applying a bias voltage. The energy and directionality of ions are affected by the substrate bias voltage. To obtain specific facial modification, the sample can be simply tilted into a certain direction. As a consequence, the surface or face of pillars that is irradiated by Ar-ion beam has distinct characteristics compared to shadowed parts of the opposing face on the same pillar.

The bending mechanism of pillars in broad ion beam irradiation process is different from e-beam irradiation. Depending on the material and energy of ion beam, surface may undergo chemical reaction upon exposure to energetic ions which alter the physical properties of the surface. On polydimethylsiloxane (PDMS), Ar-ion beam irradiation would create a stiffening process on the surface by polymeric chain-scissoring process of oxygen and carbon bond, resulting in a SiO_x-rich PDMS surface. A thin skin with stiffness $\sim$100 times higher than PDMS was observed in the compressive stress state [47,48]. To release the stress, the stiff

skin would shrink to form wrinkles and squeeze the irradiated surface. Furthermore, with the increase of the ion beam irradiation duration, a material loss would occur due to sputtering of polymer material induced from continuous bombardment of ion beam, which accompanies shrinkage on the ion beam facing side of the pillar. Finally, the vertical pillars are bent towards the irradiation direction. The tilt angle was found to change from 0° to 32°. An SEM image of Janus-faced micropillars fabricated using the broad ion beam irradiation process is shown in Figure 4(b).

In the case of PDMS with Ar-ion beam irradiation for time duration of t, using acceleration voltage of 1 keV, and a bias voltage of −600 V, the local shrinkage ε is given by the relation $\varepsilon \cong 0.57$t. The theoretical tilt angle θ due to the local shrinkage, ε is given by [29]:

$$\theta = \varepsilon\left(\frac{h}{d}\right), \tag{2}$$

here, h and d are the height and diameter of pillar, respectively. It is important to note that the angled pillars obey Equation (2) to certain time duration. After a certain treatment time, the bending angle was no longer linearly related to the treatment duration. The reason can be attributed to the dominance of etching effect over stiffening process at long irradiation times, and therefore the tilt angle is relatively independent of treatment duration.

The irradiation process using broad ion beam offers a high yield with fast processing and good uniformity. The tilted pillar structures after broad ion beam irradiation can further be integrated with chemical face modification [30]. The limitation of broad ion beam irradiation process is the requirement of vacuum process with high initial costs.

3.3. *Oblique metal deposition*

As an alternative to e-beam or ion beam irradiation, oblique or glancing angle deposition of metals has been introduced recently [32,34,42,43]. Oblique metal deposition on polymeric pillars is a versatile process to make angled HAR pillars as it is possible to cover large area, is a fast process, and uniform yields are obtained. The process is also relatively simple and featured with the controllability in tilt angle and direction of HAR pillars. In this process, a thin metallic film is deposited by tilting the sample with vertical pillars. The metal-coated pillars possess different properties in term of surface energy and modulus of elasticity on the two sides. Depending on the nature of metal film, thickness, and deposition process, the as-coated pillars can show an auto-bending phenomenon, which is associated with the residual stress releasing process of the deposited film on the pillars. In general, a metal film deposited with high energetic process such as thermal evaporation or sputtering will have residual stress either in tensile or compressive state [49]. Here, to release the generated stress in the film after deposition, geometry change compensation should arise as the film is constrained by the polymer substrate. This mechanism is further expressed by a contraction or expansion, depends on the residual stress state of a single side of the pillar, which result in bending pillar structure with certain tilt angle. The minimum thickness of the film to show auto bending was reported to be 20 nm in the case of PUA pillars coated with Au and Al with thermal evaporation process [43]. Taking the advantage of the bending characteristics in the system of oblique metal deposition process on polymeric pillars, one can further exploit the control of face selection of the Janus-faced structures.

To further amplify the bending curvature of the Janus-faced pillars through oblique metal deposition method, a second process of annealing is required when the film is very thin (less than 15 nm). The exposure of samples to high temperature allows the two different materials

to expand differently. As they have different expansion coefficients, vertical pillars will be bent to the side with larger expansion coefficient with permanent plastic deformation. When sample is cooled, the two materials shrink but the deformed or stooped state of the sample remains.

Yoon and co-workers suggested a simple oblique Pt deposition on PUA nanopillars using a Pt ion coater [32]. By tilting the sample holder to a certain angle, only one side of the pillar was coated with Pt. Because of low deposition energy of standard Pt ion coater in the SEM system, the stress generated in the film was low so that no bending was observed initially. During the subsequent annealing process at high temperature, the metallic face with larger thermal expansion coefficient expands causing thermal expansion mismatch at the interface. As the temperature decreases during cooling, the metal film shrinks at a larger strain (ratio of volume change to initial volume) rate compared to native polymer substrate with the residual stress produced being in compressive state. Therefore, the pillars were angled to the direction of metal face. The SEM image of Janus-faced structures produced by this process is shown in Figure 4(c). It was found that the angle was highly dependent on the annealing temperature and time [32].

More recently, Chu and co-workers reported an alternative method to bend metallic nanopillars by using oblique gold deposition. [42]. Here, a set of Si vertical pillars were obliquely deposited with a thin gold film by e-beam-assisted thermal evaporation. The hot gold atoms condensed on the Si pillars were in tensile residual stress during the deposition. Meanwhile, the Si pillars were heated by the hot gold atoms that condensed on the surface. When the coated sample was cooled down to room temperature, the combination of the residual stress in the gold film with the thermal residual stress in the Si pillars from the thermal expansion mismatch between gold film and Si pillars made the vertical Si pillars angled.

3.4. Angle directionality of Janus-faced pillars

The physical modification of Janus-faced pillars using broad ion beam and e-beam irradiation produced a permanent bending of the structures towards the beam direction. However, using metallic film deposition, it is possible to control the bending direction by applying different metals when the film is relatively thick. For example, Au films would make the pillars bend towards the metal-coated face. However, Al coating would make the pillars bend oppositely towards the polymeric face. This phenomenon is depend on the state of residual stress in the metallic film deposited on the pillars (i.e. a tensile residual stress will bend the pillars towards the film side, while a compressive residual stress will bend the pillars towards the polymer side) [43]. The intrinsic stress of most metallic films deposited with evaporation or ion bombardment is in tensile state [49]. During thermal evaporation, the individual metal atoms are in tensile state due to larger thermal expansion coefficient relatively to the polymer substrate. When a metal is deposited on the substrate with lower temperature, the metal film will contract to pull the pillars towards the metal face as the metal film is confined by the polymer substrate. On the other hand, for specific reactive metals such as Al, the impurities in the film can easily modify the stress state into compression. The mechanisms can be attributed to direct diffusion of interstitial impurities, compound formation in the grain boundaries, and impurities absorption below the top surface of the growing films [49]. Figure 5 shows the face selection in Janus-faced pillars based on the residual state in the film.

Another way to control the bending direction is the additional process using chemical decomposition by e-beam irradiation [32]. Once tilted Janus-faced structures were made either by metallic coating or ion beam irradiation, the subsequent e-beam irradiation on the unex-

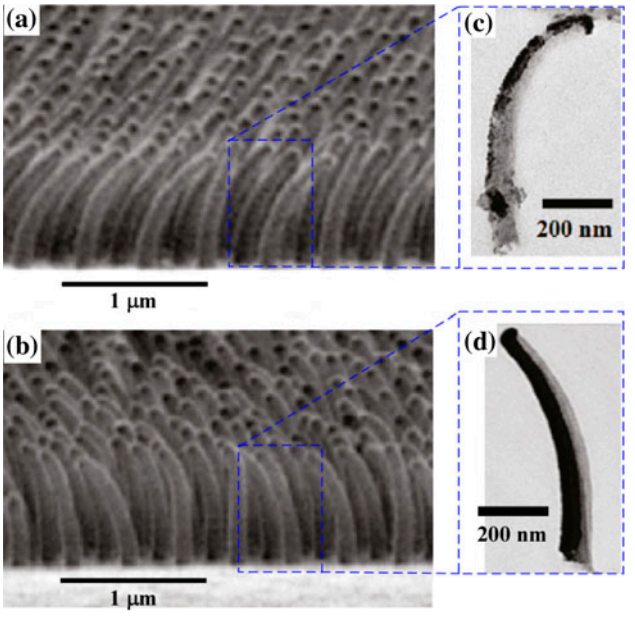

Figure 5. Face selection in Janus-faced pillar structures based on the residual stress state in the film: (a) compressive and (b) tensile. The transmission electron microscopy (TEM) images of metallic films on native PUA pillars deposited by thermal evaporation: (c) an Al film on PUA shows a compressive stress, therefore, the pillars bent towards the polymer face direction. On the other hand, (d) an Au film on PUA shows a tensile stress, therefore, the pillars bent towards the film face direction. Images are reprinted from [43].

posed face will induce shrinkage in the irradiated part. As the result, the bending direction of Janus-face structures can be flipped to the opposite face direction.

3.5. *Post-treatment of Janus-faced structures after physical modification*

In nanoscale adhesion, the work of adhesion depends on the surface energy of the contacting materials. After conducting physical deposition on the selected face of micro or nanopillars, Janus-faced structures can be varied in surface energy with chemical face modification. In this case, the tilted samples with vertical or pre-bent pillars are exposed to ion beam irradiation, which increases the surface energy of the exposed surface [30]. In our recent work, oxygen ion beam was utilized to alter the surface energy of polymer pillars. Depending on the duration of ion beam irradiation, the chemical reaction was controlled to induce the oxidation only while preventing the etching process. Using the PUA sample, X-ray photoelectron spectroscopy (XPS) measurement showed that the profile of radicals (C^*) in the linear chain of ($–[C^*H_2–CH_2]_n–$) backbone in the PUA materials were increased as well as the –CO, and –COO bonds (data not shown). It is indicative that the oxygen ion beam breaks the carbon chains backbone and oxidizes the substrate, resulting in a significant increase in the apparent surface energy [30].

A brief summary for the comparison of available fabrication methods for Janus-faced structures is presented in Table 2. From the table, it is apparent that both physical and chemical face modifications offer complementary avenues for optimum design of artificial dry adhesives.

Table 2. Comparison of Janus-faced structure characteristics using various methods.

	Physical face modification			Chemical face modification
	E-beam	Ion beam	Oblique metal deposition	Chemical vapour deposition
Fabrication process	Two-step: molding + irradiation	Two-step: molding + irradiation	Three-step: molding + metal coating + annealing	Three-step: molding, irradiation, oblique CVD
Coverage area	Very small	Large	Large	Large
Fabrication speed	Slow	Fast	Fast	Fast
Shape and morphology	Non-uniform	Uniform	Uniform	Uniform
Changes in mechanical properties	Negligible	Depends on exposure time	Yes	Negligible
Changes in chemical properties	Negligible	Depends on exposure time	Yes	Yes
Maximum tilt angle (deg.)	30	80	20	NA
Modification state	Permanent	Permanent	Pseudo-permanent	Reversible to permanent

Note: NA – Not applicable.

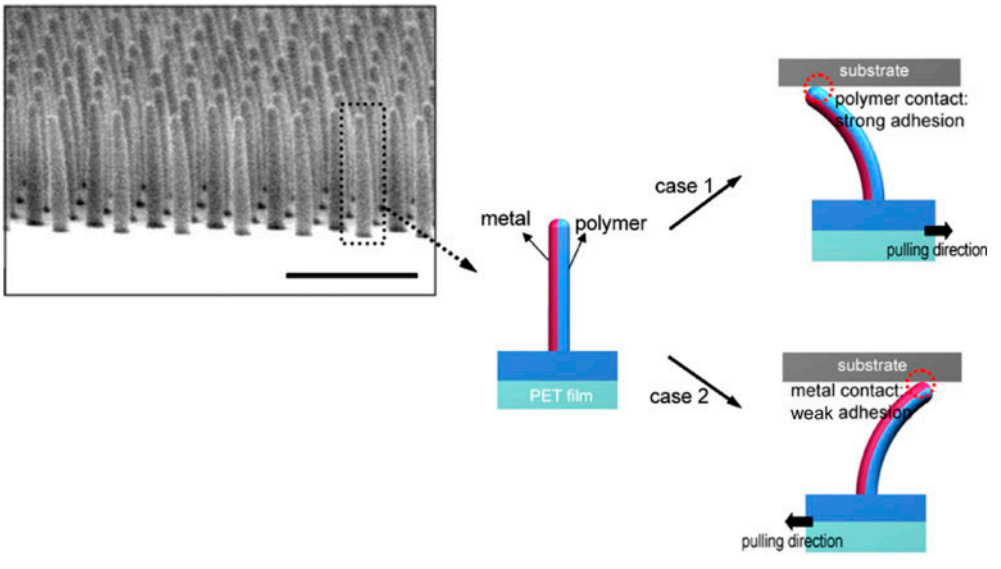

Figure 6. The vertical pillars with Pt coating on one side and native polymer on the other side. The scheme shows the directional shear adhesion along the pulling direction. Reprinted from [32].

4. Adhesion properties of Janus-faced structures

4.1. Role of work of adhesion

The adhesion properties of Janus-faced structures are different on the two opposing faces due to mechanical and chemical differences. Yoon and co-workers studied the macroscopic adhesion force and directional adhesion hysteresis with Janus-faced nanopillars (Pt film coated on PUA pillars) [32]. After oblique angle deposition of Pt film on vertically aligned PUA nanopillars, the shear adhesion force tests were conducted in such a way that the shear direction was parallel to the Pt film face in the first case and to polymer face in the other case. Figure 6 shows the SEM image of the Pt coated PUA nanopillars and the directions of shear adhesion force test.

The directional sensitivity of Janus-faced nanopillars can be attributed to material properties of the Janus structures brought into contact with the test surface. The general relationship on the effect of surface properties and work of adhesion can be explained, for example, by the harmonic mean equation. When two different materials are in contact, the work of adhesion, W_{12} is given by [50]:

$$W_{12} = 4\left(\frac{\gamma_1^d \gamma_2^d}{\gamma_1^d + \gamma_2^d} + \frac{\gamma_1^p \gamma_2^p}{\gamma_1^p + \gamma_2^p}\right), \tag{3}$$

Here, the superscripts d and p are the dispersion and polar components of surface tension γ, respectively. The surface tension force can be measured from the wetting angle on flat sample using polar and nonpolar probe liquids. The probe liquids of de-ionized water and formamide were used for polar and dispersion components measurement, respectively, using the Owens–Wendt method [51]. It was observed that the intrinsic surface energy of nanohairy structures, widely controlled from 21.3 to 72.8 mJ/m^2, was shown to increase the adhesion strength by more than fivefold as shown in Figure 7.

4.2. Role of tilt angle

In general, it is reasonable to expect that the shear adhesion force is highly dependent on the contact length of pillar geometry which is varied by the tilt angle of the pillars. However, the direct determination of actual contact length is not easy with the current approaches, espe-

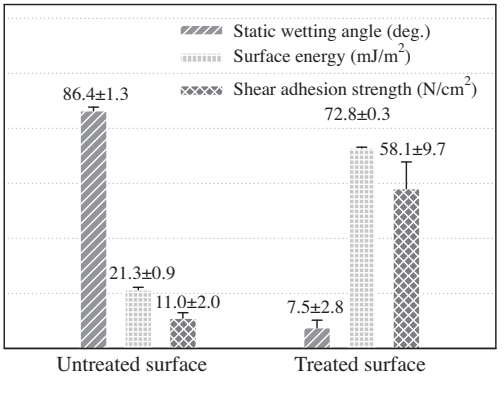

Figure 7. Effects of oxygen ion beam treatment on the PUA surface properties: static wetting angle, surface energy, and shear adhesion strength. Redrawn from [30].

cially when the pillar size is in nanoscale. With Equation (3) together with macroscopic shear adhesion force measurements, the work of adhesion between Janus-faced pillar surface and test substrate, W_{12} can be used to estimate the contact length of the system. By considering the Janus-faced pillars as elastic solids and using the Johnson–Kendall–Roberts theory [52], the contacting Janus-faced pillar surface makes a square interface with the length L_c and contact width W_c expressed by [53,54]:

$$W_c = 8\left\{\frac{(1-\upsilon^2)R^2W_{12}}{\pi E}\right\}^{1/3}, \tag{4}$$

here, υ and R are the Poisson's ratio and radius of pillar, respectively. The shear adhesion force of a single pillar can be expressed as [53–55]:

$$F_s = A\tau = W_c L_c \tau, \tag{5}$$

where τ is the interfacial shear strength of the pillar and L_c is the contact length induced by the leaning angle of pillar. Finally, one can estimate the actual contact length from the macroscopic shear adhesion force of the sample. Jeong and co-workers showed that the contact length induced by tilt angle has a linear profile with respect to shear adhesion [53]. It was estimated that increasing tilt angle from zero to 45° produced about fourfold increase in shear adhesion strength [53].

A more general viewpoint on the effect of tilt angle and aspect ratio of pillar structures is shown in Figure 8. Here, to describe the general adhesion performance regardless of the scale (in micro or nanoscale), the adhesion strength is represented by the pull-off strength (the normal adhesion force per unit contact area). As shown, for pillar structures of the same material,

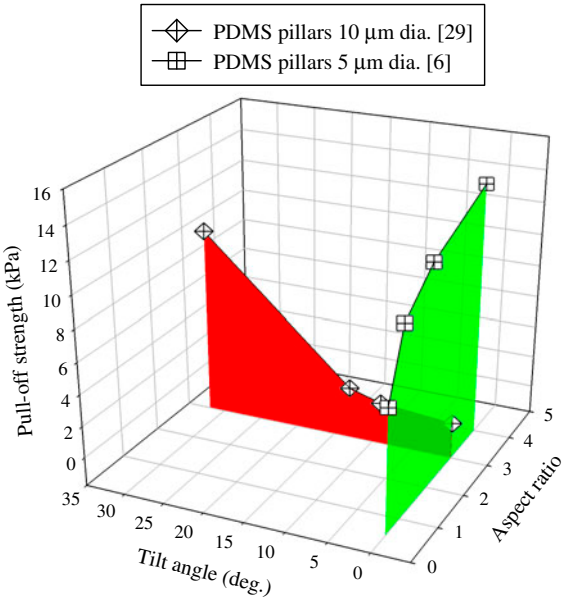

Figure 8. The pull-off strength profile as a function of tilt angle and aspect ratio of angled, HAR structures.

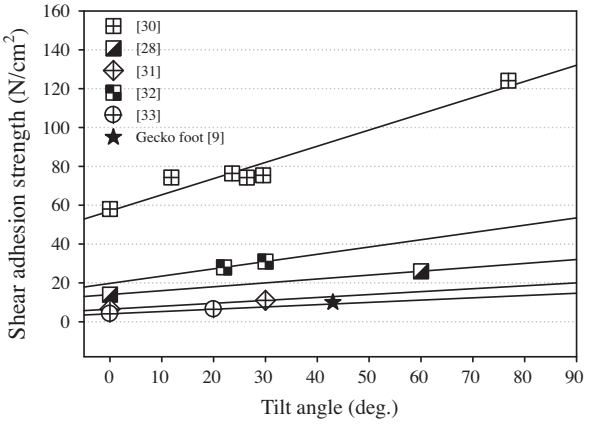

Figure 9. Plot of shear adhesion strength of various angled HAR structures. A linear profile of shear adhesion strength is attributed to the linear increase of contact length induced by increasing tilt angle. The star symbol represents the shear adhesion strength and tilt angle of real gecko foot for comparison. A remarkable increase in shear adhesion strength in [30] is attributed to the using of high-surface energy materials.

an increase in tilt angle would give approximately an exponential rise in the pull-off strength. On the other hand, an increase in aspect ratio would give approximately a logarithmic rise in the pull-off strength.

A brief summary on the dependency of shear adhesion strength on tilt angle of HAR structures is shown in Figure 9. Here, the shear adhesion strength and tilt angle of spatula in real gecko foot is shown for comparison. The shear adhesion strength can be calculated empirically from the shear adhesion force of the individual pillar in Equation (5) (multiplied by the total number of pillars per unit area). In general, it is observed that the measured shear adhesion strength is lower than the theoretical calculation due to existence of defects in the structures or inaccurate estimation of τ [30,53]. It can be seen clearly from Figure 9 that the contact length induced by tilt angle has a linear profile with respect to the shear adhesion force and, therefore, the shear adhesion strength.

From the analysis of adhesion properties discussed above, the control of surface energy and tilt angle is a key factor in designing high adhesion strength artificial dry adhesives. It is also obvious that Janus-face structures can provide versatile options for simultaneous control of tilt angle and surface energy for angled micro and nanopillars.

4.3. Adhesion hysteresis in Janus-faced structures

The unique properties of Janus-faced structures enable one to amplify the difference in adhesion strength in the two opposing face directions. In particular, we can expect that adhesion hysteresis on Janus-faced structures would be very high towards the angled face and significantly low in the opposite face [32]. Such unidirectional or anisotropic adhesion property of Janus-faced structures is an important feature for optimum design of a smart adhesive system with high adhesion and easy detachment.

Figure 10 shows the summary of adhesion hysteresis of various systems having Janus-faced structures. In particular for PUA/Pt Janus system with vertical nanopillars, the maxi-

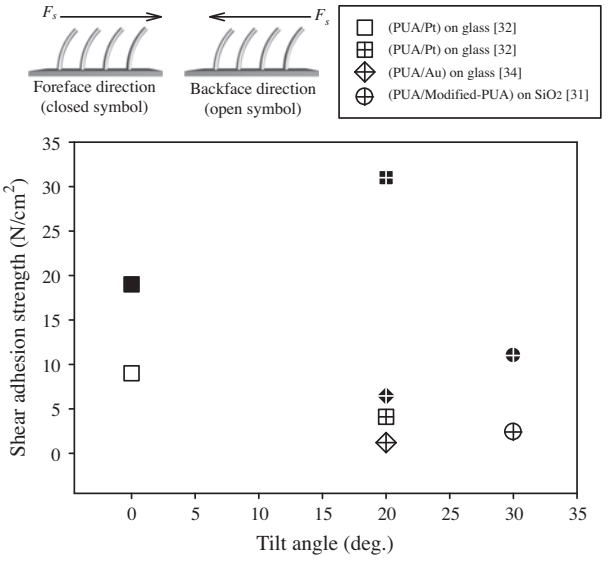

Figure 10. Comparison of adhesion hysteresis, the difference in shear adhesion strength by foreface and backface pulling force direction, of various Janus-faced pillars with different tilt angles and test surfaces. The direction of shear adhesion strength is shown in the scheme (the closed and open symbols indicate the foreface and backface pulling force directions, respectively).

mum adhesion strength is about 18 N/cm^2 in the foreface direction (PUA face direction), while the maximum adhesion strength in the backface direction (Pt face direction) is about 9 N/cm^2. On the same Janus-faced system of PUA/Pt with angled structures, the maximum adhesion strength is elevated to 31 N/cm^2 in the foreface direction and about 4 N/cm^2 in the backface direction. This result shows that the tilt angle of pillar structures plays a key role in increasing the shear adhesion strength as well as to amplify the adhesion hysteresis.

5. Conclusion

We have presented recent developments on a new class of artificial dry adhesives based on Janus-faced micro and nanopillars. The unique properties of Janus-faced structures can be exploited in terms of surface chemistry and geometry aspects. The fabrication method for Janus-faced structures mainly involves a certain type of physical modification in the form of e-beam irradiation, broad ion beam irradiation, and oblique metal deposition. The physical modification offers permanent or pseudo-permanent deformation to the as-prepared vertical pillars that are typically made by conventional photolithography and/or soft lithography by replica molding. The bending mechanism is quite different for each method by utilizing, for example, volumetric shrinkage, formation of a skin layer in the stiffening process, and difference in the thermal expansion coefficients. After the physical modification, the surface of angled micro and nanopillars can further be tuned to have a higher surface energy or a different surface roughness. It appears that the fabrication techniques presented in this review are relatively complicated especially for angled nanopillars, typically involving multistep processes. A trade-off generally arises between the quality of resulting structures and cost issues.

Therefore, it is advised that a suitable fabrication technique should be selected considering the material properties and desired adhesion performance.

It was shown that several unique features in Janus-faced structures are useful for artificial dry adhesives. First, the structures provide the flexible design and control of pillar shape and tilt angle, which are of great importance to high shear adhesion strength as well as high adhesion hysteresis. Also, the distinct contrasts in physical and chemical properties on the opposing sides of Janus-faced structures are potentially useful for other applications such as directional wetting and friction. Overall, it can be seen that Janus-faced structures have the potential to be an efficient system in realizing the optimum design of artificial dry adhesives.

Acknowledgments

We gratefully acknowledge support from National Research Foundation of Korea (NRF) grant (No. 20110017530), WCU (World Class University) program (R31-2008-000-10083-0), and Basic Science Research Program (2010-0027955). This work was also supported, in part, by the Korea Research Foundation Grant (KRF-J03003), Korea Institute of Science and Technology (KIST) Internal Project, and the Institute of Biological Engineering of Seoul National University.

References

[1] Irschick DJ, Austin CC, Petren K, Fisher RN, Losos JB, Ellers O. A comparative analysis of clinging ability among pad-bearing lizards. Biological Journal of the Linnean Society. 1996;59:21–35.

[2] Arzt E, Gorb S, Spolenak R. From micro to nano contacts in biological attachment devices. Proceedings of the National Academy of Sciences USA. 2003;100:10603–6.

[3] Ruibal R, Ernst V. The structure of the digital setae of lizards. Journal of Morphology. 1965;117:271–94.

[4] Autumn K, Hansen W. Ultrahydrophobicity indicates a non-adhesive default state in gecko setae. Journal of Comparative Physiology A. 2006;192:1205–12.

[5] Huber G, Mantz H, Spolenak R, Mecke K, Jacobs K, Gorb SN, Arzt E. Evidence for capillarity contributions to gecko adhesion from single spatula nanomechanical measurements. Proceedings of the National Academy of Sciences USA. 2005;102:16293–6.

[6] Greiner C, del Campo A, Arzt E. Adhesion of bioinspired micropatterned surfaces: Effects of pillar radius, aspect ratio, and preload. Langmuir. 2007;23:3495–502.

[7] Autumn K, Liang YA, Hsieh ST, Zesch W, Chan WP, Kenny TW, Fearing R, Full RJ. Adhesive force of a single gecko foot-hair. Nature. 2000;405:681–5.

[8] Hansen WR, Autumn K. Evidence for self-cleaning in gecko setae. Proceedings of the National Academy of Sciences USA. 2005;102:385–9.

[9] Autumn K, Majidi C, Groff RE, Dittmore A, Fearing R. Effective elastic modulus of isolated gecko setal arrays. Journal of Experimental Biology. 2006;209:3558–68.

[10] Kim TW, Bhushan B. Adhesion analysis of multi-level hierarchical attachment system contacting with a rough surface. Journal of Adhesion Science and Technology. 2007;21:1–20.

[11] Santos D, Spenko M, Parness A, Kim S, Cutkosky M. Directional adhesion for climbing: theoretical and practical considerations. Journal of Adhesion Science and Technology. 2007;21:1317–41.

[12] Dahlquist CA, Patrick RL, editor. Treatise on adhesion and adhesives. New York, NY: Marcel Dekker; 1969. 219–60.

[13] Persson BNJ. Biological adhesion for locomotion: basic principles. Journal of Adhesion Science and Technology. 2007;21:1145–73.

[14] Majumder A, Ghatak A, Sharma A. Microfluidic adhesion induced by subsurface microstructures. Science. 2007;318:258–61.

[15] Ghatak A, Mahadevan L, Chung JY, Chaudhury MK, Shenoy V. Peeling from a biomimetically patterned thin elastic film. Proceedings of the Royal Society A. 2004;460:2725–35.
[16] del Campo A, Greiner C, Alvarez I, Arzt E. Patterned surfaces with pillars with controlled 3D tip geometry mimicking bioattachment devices. Advanced Materials. 2007;19:1973–7.
[17] Gorb SN, Varenberg M. Mushroom-shaped geometry of contact elements in biological adhesive systems. Journal of Adhesion Science and Technology. 2007;21:1175–83.
[18] Murphy MP, Aksak B, Sitti M. Gecko-inspired directional and controllable adhesion. Small. 2009;5:170–5.
[19] Gao HJ, Yao HM. Shape insensitive optimal adhesion of nanoscale fibrillar structures. Proceedings of the National Academy of Sciences USA. 2004;101:7851–6.
[20] Autumn K, Sitti M, Liang YCA, Peattie AM, Hansen WR, Sponberg S, Kenny TW, Fearing R, Israelachvili JN, Full RJ. Evidence for van der Waals adhesion in gecko setae. Proceedings of the National Academy of Sciences USA. 2002;99:12252–6.
[21] Greiner C, Spolenak R, Arzt E. Adhesion design maps for fibrillar adhesives: the effect of shape. Acta Biomaterialia. 2009;5:597–606.
[22] Aksak B, Murphy MP, Sitti M. Adhesion of biologically inspired vertical and angled polymer microfiber arrays. Langmuir. 2007;23:3322–32.
[23] Murphy MP, Aksak B, Sitti M. Adhesion and anisotropic friction enhancements of angled heterogeneous micro-fiber arrays with spherical and spatula tips. Journal of Adhesion Science and Technology. 2007;21:1281–96.
[24] Reddy S, Arzt E, del Campo A. Bioinspired surfaces with switchable adhesion. Advanced Materials. 2007;19:3833–7.
[25] Gates BD, Xu Q, Love JC, Wolfe DB, Whitesides GM. Unconventional anofabrication. Annual Review of Materials Research. 2004;34:339–72.
[26] Rogers JA, Lee HH. Unconventional Nanopatterning Techniques and Applications. Hoboken, NJ: Wiley; 2008.
[27] Lee JH, Fearing RS, Komvopoulos K. Directional adhesion of gecko-inspired angled microfiber arrays. Applied Physics Letters. 2008;93:191910.
[28] Jeong HE, Lee JK, Kim HN, Moon SH, Suh KY. A nontransferring dry adhesive with hierarchical polymer nanohairs. Proceedings of the National Academy of Sciences USA. 2009;106:5639–44.
[29] Moon MW, Cha TG, Lee KR, Vaziri A, Kim HY. Tilted janus polymer pillars. Soft Matter. 2010;6:3924–9.
[30] Rahmawan Y, Kim TI, Kim SJ, Lee KR, Moon MW, Suh KY. Surface energy tunable nanohairy dry adhesive by broad ion beam irradiation. Soft Matter. 2012;8:1673–80.
[31] Kim TI, Jeong HE, Suh KY, Lee HH. Stooped nanohairs: geometry-controllable, unidirectional, reversible, and robust gecko-like dry adhesive. Advanced Materials. 2009;21:2276–81.
[32] Yoon H, Jeong HE, Kim TI, Kang TJ, Tahk D, Char K, Suh KY. Adhesion hysteresis of janus nanopillars fabricated by nanomolding and oblique metal deposition. Nano Today. 2009;4:385–92.
[33] Kim TI, Pang C, Suh KY. Shape-tunable polymer nanofibrillar structures by oblique electron beam irradiation. Langmuir. 2009;25:8879–82.
[34] Choi MK, Yoon H, Lee K, Shin K. Simple fabrication of asymmetric high-aspect-ratio polymer nanopillars by reusable AAO templates. Langmuir. 2011;27:2132–7.
[35] Han M, Lee W, Lee SK, Lee SS. 3D microfabrication with inclined/rotated UV lithography. Sensors Actuators A. 2004;111:14–20.
[36] Elsner H, Meyer HG. Nanometer and high aspect ratio patterning by electron beam lithography using a simple DUV negative tone resist. Microelectronic Engineering. 2001;57–58:291–6.
[37] Geim AK, Dubonos SV, Grigorieva IV, Novoselov KS, Zhukov AA, Shapoval SY. Microfabricated adhesive mimicking gecko foot-hair. Nature Materials. 2003;2:461–3.

[38] Vasile MJ, Nassar R, Xie JS. Focused ion beam technology applied to microstructure fabrication. Journal of Vacuum Science and Technology B. 1998;16:2499–505.
[39] Fu Y, Bryan NKA. Fabrication and characterization of slanted nanopillars array. Journal of Vacuum Science and Technology B. 2005;23:984–9.
[40] Pokroy B, Kang SH, Mahadevan L, Aizenberg J. Self-organization of a mesoscale bristle into ordered, hierarchical helical assemblies. Science. 2009;323:237–40.
[41] Chandra D, Yang S. Stability of high-aspect-ratio micropillar arrays against adhesive and capillary forces. Accounts of Chemical Research. 2010;43:1080–91.
[42] Chu KH, Xiao R, Wang EN. Uni-directional liquid spreading on asymmetric nanostructured surfaces. Nature Materials. 2010;9:413–7.
[43] Yoon H, Woo H, Choi MK, Suh KY, Char K. Face selection in one-step bending of janus nanopillars. Langmuir. 2010;26:9198–201.
[44] Choi SJ, Yoo PJ, Baek SJ, Kim TW, Lee HH. An ultraviolet-curable mold for sub-100-nm lithography. Journal of the American Chemical Society. 2004;126:7744–5.
[45] Azuma T, Chiba K, Abe H, Motoki H, Sasaki N. Mechanism of ArF resist-pattern shrinkage in critical-dimension scanning electron microscopy measurement. Journal of Vacuum Science and Technology B. 2004;22:226–30.
[46] Ahmed SF, Yi JW, Moon MW, Jang YJ, Park BH, Lee SH, Lee KR. The morphology and mechanical properties of polycarbonate/acrylonitrile butadiene styrene modified by ar ion beam irradiation. Plasma Processes and Polymers. 2009;6:860–5.
[47] Ahmed SF, Rho GH, Lee KR, Vaziri A, Moon MW. High aspect ratio wrinkles on a soft polymer. Soft Matter. 2010;6:5709–14.
[48] Moon MW, Lee SH, Sun JY, Oh KH, Vaziri A, Hutchinson JW. Wrinkled hard skins on polymers created by focused ion beam. Proceedings of the National Academy of Sciences USA. 2007;104:1130–3.
[49] Dheurle FM, Harper JME. Note on the origin of intrinsic stresses in films deposited via evaporation and sputtering. Thin Solid Films. 1989;171:81–92.
[50] Wu S. Polar and nonpolar interactions in adhesion. Journal of Adhesion. 1973;5:39–55.
[51] Owens DK, Wendt RC. Estimation of the surface free energy of polymers. Journal of Applied Polymer Science. 1969;13:1741–7.
[52] Johnson KL, Kendall K, Roberts AD. Surface energy and the contact of elastic solids. Proceedings of the Royal Society of London, Series A: Mathematical and Physical Sciences. 1971;324:301–13.
[53] Jeong HE, Lee JK, Kwak MK, Moon SH, Suh KY. Effect of leaning angle of gecko-inspired slanted polymer nanohairs on dry adhesion. Applied Physics Letters. 2010;96:043704.
[54] Majidi CS, Groff RE, Fearing RS. Attachment of fiber array adhesive through side contact. Journal of Applied Physics. 2005;98:103521.
[55] Homola AM, Israelachvili JN, McGuiggan PM, Gee ML. Fundamental experimental studies in tribology - the transition from interfacial friction of undamaged molecularly smooth surfaces to normal friction with wear. Wear. 1990;136:65–83.